

Does export production measure transient changes of the biological carbon pump under global warming?

Wolfgang Koeve¹, Paul Kähler¹, and Andreas Oschlies¹

¹Helmholtz-Zentrum für Ozeanforschung Kiel, GEOMAR

November 22, 2022

Abstract

In a widely-held conception, the biological carbon pump (BCP) is equal to the export of organic matter out of the euphotic zone. Using global ocean-atmosphere model experiments we show that the change in export production is a poor measure of the biological pump's feedback to the atmosphere. The change in global true oxygen utilization (TOU), an integrative measure of the imprint of the biological carbon pump on marine oxygen, however, is in good agreement with the net change in the biogenic air-sea flux of oxygen. Since, TOU correlates very well with apparent oxygen utilization (AOU) in our experiments, we propose to measure the change of AOU from data of global float programs to monitor the feedback of the BCP to the atmosphere. For the current ocean we estimate that BCP changes lead to an uptake of CO by the ocean in the range of 0.07 to 0.14 GtC/yr.

Fig. 3

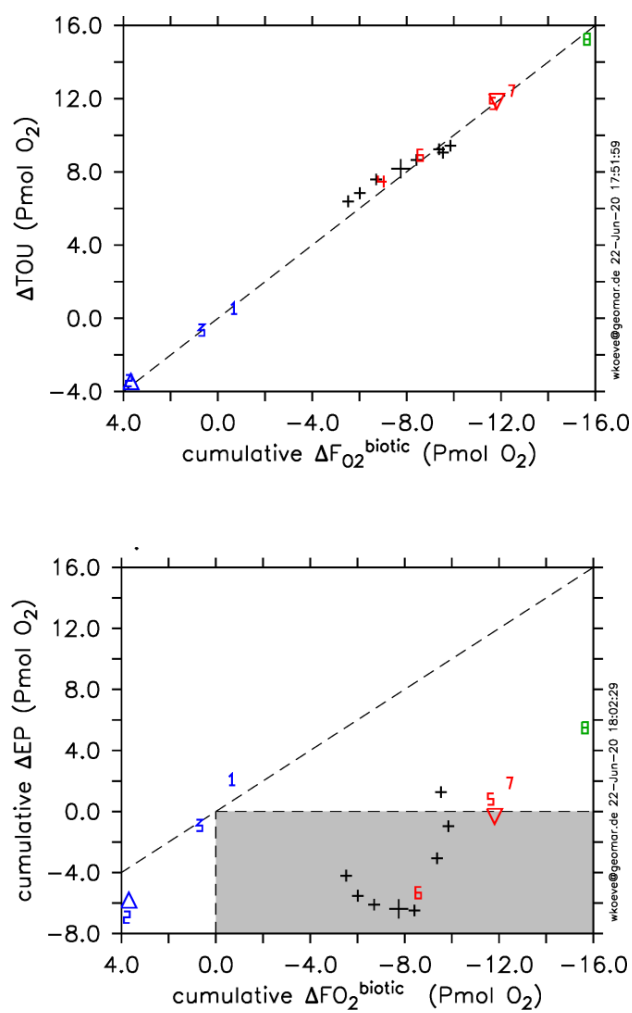
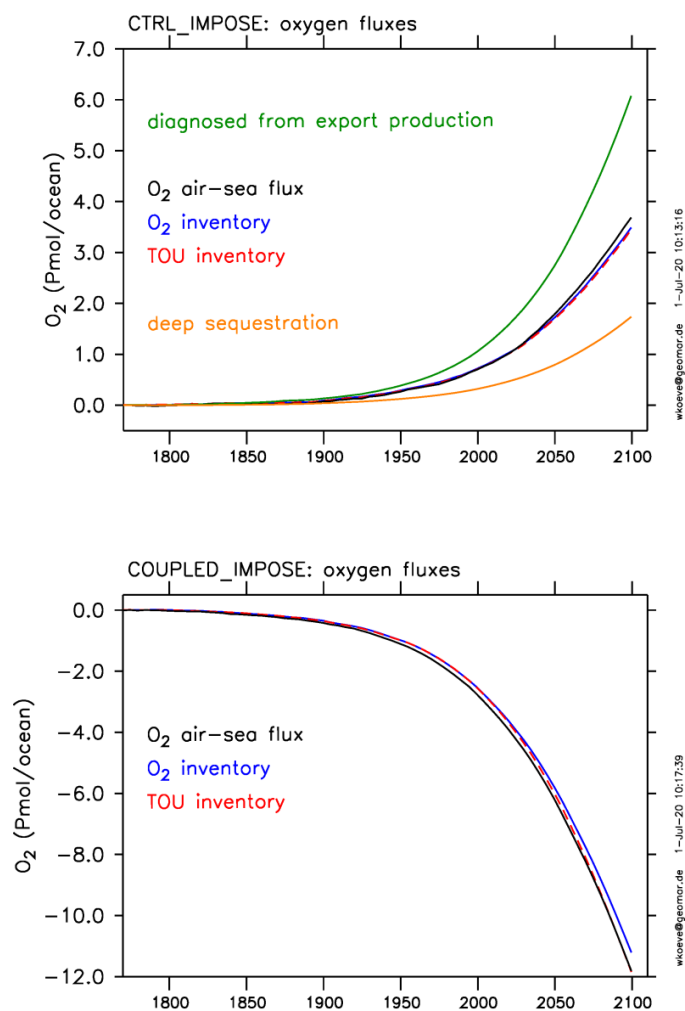


Fig. 2



Does export production measure transient changes of the biological carbon pump under global warming?

Koeve¹, W., Kähler¹, P., Oschlies¹, A.

¹ Biogeochemical Modelling, Helmholtz-Zentrum für Ozeanforschung Kiel (GEOMAR), Kiel, Germany

Correspondence to: W. Koeve (wkoeve@geomar.de)

1. Plain language summary:

The biological carbon pump is an important element of marine carbon cycling and climate control on millennium time scales. In a widely-held conception the export of organic carbon from the productive surface layer of the ocean is used as the essential measure of this carbon pump. Using numerical ocean modelling, we show here that the change in export production is, however, a poor measure of the biological carbon pump's feedback to the atmosphere on centennial time scales. In the contrary, we find that an oxygen-based measure, the apparent oxygen utilization can be used to quantify the impact of biological pump changes on the atmosphere. Since the apparent oxygen utilization is easily accessible from an existing network of marine floats, our study suggests that the atmospheric impact of any future changes of the biological carbon pump can be monitored and quantified. For past decades our study proposes a neglectable CO₂-feedback to climate from biological carbon processing.

2. Abstract/first paragraph

In a widely-held conception, the biological carbon pump (BCP) is equal to the export of organic matter out of the euphotic zone. Using global ocean-atmosphere model experiments we show that the change in export production is a poor measure of the biological pump's feedback to the atmosphere. The change in global true oxygen utilization (TOU), an integrative measure of the imprint of the biological carbon pump on marine oxygen, however, is in good agreement with the net change in the biogenic air-sea flux of oxygen. Since, TOU correlates very well with apparent oxygen utilization (AOU) in our experiments, we propose to measure the change of AOU from data of global float programs to monitor

the feedback of the BCP to the atmosphere. For the current ocean we estimate that BCP changes lead to an uptake of CO₂ by the ocean in the range of 0.07 to 0.14 GtC/yr.

3. Introduction

The biological carbon pump (hereafter BCP, also coined soft tissue pump, [Volk and Hoffert, 1985]) is often equated with the export of organic matter out of the euphotic zone [Boyd and Trull, 2007; Harrison *et al.*, 2018; Keeling *et al.*, 2010; Yool *et al.*, 2007]. Attempts to quantify the ‘efficiency’ or the ‘strength’ of the biological pump often use export production as its essential measure. The fraction of net primary production vertically exported from the surface layer has been explored extensively in its relationships with temperature, nutrient availability, or net primary productivity, and with respect to its global patterns [Buesseler, 1998; Eppley and Peterson, 1979; Henson *et al.*, 2012; Henson *et al.*, 2011; Laws *et al.*, 2000]. In climate models, net primary production and export production have been used to quantify changes of marine ecosystems and the reaction of the biological pump to future climate change [Cabre *et al.*, 2015; Laufkötter *et al.*, 2016; Laufkötter *et al.*, 2015; Taucher and Oschlies, 2011]. Models consistently projects a decrease of global export production (EP) by on average 12 % ($\Delta EP = -0.68 \pm 0.54$ GtC/yr) until the end of this century for a business-as-usual emission scenario [Cabre *et al.*, 2015]. The ultimate drivers of this reduction are increasing density stratification [Bopp *et al.*, 2002; J. L. Sarmiento *et al.*, 1998], caused by surface ocean warming and increased moisture fluxes, and mixed layer shoaling. These physical changes reduce nutrient supply from the deep ocean, followed by decreasing net primary production, phytoplankton biomass and ultimately export [Cabre *et al.*, 2015], in particular in the low latitudes, while export increases in the high latitudes. The projected net global decrease in export production has been suggested to potentially sustain a positive feedback to atmospheric CO₂ concentrations [Cabre *et al.*, 2015], i.e. to potentially amplify climate change [Resplandy, 2018].

This view is contrasted by observations and model projections of a widespread ocean deoxygenation until the end of this century [Bopp *et al.*, 2013] and beyond [Oschlies *et al.*, 2019; Shaffer *et al.*, 2009; Yamamoto *et al.*, 2015]. The overwhelming part of the projected marine oxygen inventory loss until the end of this century is due to an increase in apparent

oxygen utilization (AOU) [Bopp *et al.*, 2017]. AOU is an integrative measure of the (oxic) degradation of organic matter and provides a measure of the amount of ‘respired carbon’ or ‘respiratory CO₂’ [Keeling *et al.*, 2010; E. Y. Kwon *et al.*, 2011], i.e. dissolved inorganic carbon stored in the ocean interior after having been processed by the biological carbon pump [Bernardello *et al.*, 2014; Körtzinger *et al.*, 1998; Peng *et al.*, 1998]. A global increase in AOU is consistent with a net O₂ flux out of the ocean and a net CO₂ flux into the ocean, hence a negative feedback to rising atmospheric CO₂. This proposes that global-warming related changes of the biological carbon pump may mitigate, rather than amplify, climate change. The same or comparable climate models, hence propose contradicting responses of the BCP to climate change, only depending on the choice of the metric to quantify the change of the BCP.

In idealised steady-state model simulations, the global integral of AOU (or its stoichiometric equivalent remineralised-PO₄ inventory) shows a negative correlation with atmospheric pCO₂ [E Y Kwon *et al.*, 2009] while export production has no meaningful relationship with atmospheric pCO₂ [Gnanadesikan and Marinov, 2008], an observation which can be explained by a strong regional decoupling of export production and AOU, evident from the regional variability of the ‘sequestration efficiency’ [DeVries *et al.*, 2012]. Hence AOU rather than export production provides a good indicator of the biotically driven oceanic carbon storage in steady state, which is in agreement with the original definition of the ‘strength’ of the soft tissue pump given by [Volk and Hoffert, 1985]. However, the Holocene steady state is in transition to the Anthropocene [Crutzen, 2002a; b; Steffen *et al.*, 2011], an era of rapidly changing climate and oceans [Hoegh-Guldberg *et al.*, 2014]. On transient time scales, a change in AOU, for example in the deep ocean, may not immediately be reflected in an exchange of oxygen or CO₂ between ocean and atmosphere. For a marine process to qualify as a feedback to the atmosphere, however, an actual flux change at the air-sea boundary must occur. So far, this has neither been shown for transient changes in AOU nor for transient changes of export production.

In this paper, we use the UVic Earth System model of intermediate complexity to explore whether the cumulative change in export production or the change in AOU provide the better measure of the impact of the BCP on atmospheric O₂ and CO₂ under the transient conditions of a changing climate. Solving this question is important, if the marine feedback

to atmospheric CO₂ and climate is to be monitored and understood. We do this by comparing changes of AOU and export production with a new objective model metric, the biogenic O₂-flux between atmosphere and ocean, which we will introduce in the next section.

4. Results

Oxygen in the interior ocean can be described as the difference between preformed oxygen (O₂^{pre}) and the oxygen debt accumulated since last contact with the atmosphere from the oxidation of organic matter. We refer to this oxygen debt as true oxygen utilization (TOU), hence $O_2 = O_2^{\text{pre}} - \text{TOU}$. Preformed oxygen is the oxygen contained in sea water when it subducted from the surface into the ocean interior. It is controlled by rapid gas exchange between the surface ocean and the atmosphere, i.e. by the thermodynamic conditions of the surface ocean, its temperature and salinity, and in polar regions by the degree of ice coverage [Ito et al., 2004]. O₂^{pre} is often approximated as the saturation concentration of oxygen (O₂^{sat}) in seawater at given atmospheric pressure, surface seawater temperature and salinity. This is the concept of apparent oxygen utilization (AOU), i.e. $O_2 = O_2^{\text{sat}} - \text{AOU}$ [J L Sarmiento and Gruber, 2006].

The direct physical impact of global warming on marine oxygen, i.e. decreasing solubility with rising temperature, is usually quantified by the change of O₂^{sat} in the ocean [Ito et al., 2017; Schmidtke et al., 2017]. The change in AOU combines effects associated with changing primary production, export production, respiration, but also circulation, which ventilates (provides oxygen to) the ocean interior and thereby replaces the oxygen debt from biological processes. In an idealised ocean-atmosphere model setting, the change of the air-sea oxygen flux at the sea surface can similarly be split into a thermodynamic component ($\Delta F_{O_2}^{\text{therm}}$) related to the change in oxygen solubility (i.e. ΔO_2^{sat}), and a residual associated with ΔAOU , to the extent that it causes an oxygen flux change at the sea surface. Since this residual oxygen flux is directly or indirectly related to either the production of oxygen (net primary production) or the oxidation of organic matter (respiration), we refer to it as biogenic ($\Delta F_{O_2}^{\text{biotic}}$). $\Delta F_{O_2}^{\text{biotic}}$ includes effects from circulation slow-down which have been projected

to reduce the return flux of AOU back to the sea surface, including AOU that has been generated from organic matter breakdown long before climate change started.

In the global-warming model runs used in this study (see Suppl. Methods, Tab. S1) we explicitly exclude the thermodynamic warming component on marine oxygen by assimilating the annual mean temperature difference between a transient climate change run COUPLED and its constant climate control run CTRL (Figs. S1, S2) for the computation of oxygen gas exchange and solubility. Transient changes in simulated oxygen gas exchange between ocean and atmosphere presented in this study are hence due to $\Delta F_{O_2}^{\text{biotic}}$ only. Accordingly, we can use the biogenic oxygen air-sea flux changes as a reference metric of BCP changes in our model, against which we compare changes in (cumulative) export production and changes in AOU (TOU).

In experiment COUPLED_SST, a transient run with SST for gas exchange like in CTRL (see Tab. S1), export production decreases during the experiment (1770-2100) (Fig. S3a) while AOU and TOU, which we track by an idealised model tracer [Ito *et al.*, 2004], increase (Fig. S3b). We convert cumulative export production and TOU into equivalent oxygen flux units (Fig. 1) assuming the changes to cause an immediate flux response. Cumulative change in export production would translate into an oxygen flux from the atmosphere into the ocean (Fig. 1, green line), while the change in TOU would translate into an oxygen air-sea flux out of the ocean (Fig. 1, red line). The true biogenic oxygen air-sea flux ($\Delta F_{O_2}^{\text{biotic}}$) in COUPLED_SST (Fig. 1, black line) is out of the ocean and almost identical to the equivalent air-sea flux of the TOU change. In contrast, the theoretical O_2 -flux equivalent to the cumulative export-production change has the wrong sign compared with the modelled O_2 -flux at the air-sea boundary. This picture is consistent with earlier work [Bopp *et al.*, 2002; Yamamoto *et al.*, 2015] which showed that the direct biotic effect of reduced export production on oxygen and AOU is overcompensated by the effects of a circulation slow-down and increasing interior-ocean residence time.

We isolate the direct effects of changing biological rates from the effect of a changing circulation on tracer accumulation in experiment CTRL_IMPOSE. In this experiment, we assimilate the annual mean difference of biotic oxygen sinks-minus-sources (O_2 -sms) of

COUPLED and CTRL into a run without climate and circulation change. The globally integrated O_2 -sms in the interior ocean from this run very much resembles that of the transient climate change run COUPLED (Fig. S4a, see Supplementary Methods (S1) for details). The ocean gains oxygen in this run (globally, about 3.48 Pmol O_2 by yr 2100) (Fig. 2a), which is due to a reduction of the true oxygen utilization (TOU) (-3.46 Pmol O_2 by yr 2100). Changes in TOU and oxygen agree within 10% with a slightly larger time cumulative air-sea oxygen flux, $\Delta F_{O_2}^{biotic}$ (3.73 Pmol O_2 until yr 2100). Small differences between the cumulative $\Delta F_{O_2}^{biotic}$ and the oxygen inventory change are explained by differences in oxygen and TOU inventory changes in the upper ocean and the ocean interior (not shown), i.e. as a small hysteresis effect. Export production, the integral of O_2 -sms below 130m in this run, decreases over the course of the experiment (Fig. S3), which is consistent with an ocean gaining oxygen. However, the time-cumulative integral of export production change is larger by a factor of two (equivalent oxygen demand of 6.69 Pmol O_2 by yr 2100) compared to simulated oxygen air-sea exchange and oxygen inventory changes. This overestimate of biogenic oxygen flux by the export production metric is likely explained by shallow respiration, e.g. within the winter mixed layer [Koeve, 2001]. Organic matter sequestration flux across 1000m, sometimes suggested to better represent long term sequestration of carbon from the BCP [Barange et al., 2017; Lampitt et al., 2008], is 1.84 Pmol O_2 by yr 2100, about a factor two too low in comparison with the observed inventory changes of oxygen (or TOU), or $\Delta F_{O_2}^{biotic}$. Should a reduction of the BCP magnitude occur without circulation change it would contribute to oxygenate the ocean. In such a situation both the changes in export production and the deep ocean carbon sequestration flux ($z=1000m$) would be weak predictors of the O_2 -flux induced by the changes of the BCP, either overestimating or underestimating it by about a factor of two. However, at least the signs of change of export production, sequestration flux and the oxygen flux at the ocean-atmosphere boundary would be consistent.

We also perform the ‘counter’ experiment (COUPLED_IMPOSE), i.e. a run with changing climate and circulation in which we assimilate the annual mean difference of oxygen sinks minus sources (O_2 -sms) of COUPLED and CTRL at model run time, such that the O_2 -sms of the run COUPLED_IMPOSE very much resembles that of CTRL (Fig. S4b, see Supplementary Methods (S1) for details). In this run, again, the decrease in oxygen, the increase in TOU and

the loss of oxygen to the atmosphere ($\Delta F_{O_2}^{\text{biotic}}$) are consistent, with little hysteresis (Fig. 2b; red inverse triangle in Fig 3a). Similar to earlier work [Bopp *et al.*, 2002; Yamamoto *et al.*, 2015], the effect of circulation change on TOU (and oxygen) tracer accumulation (isolated in COUPLED_IMPOSE) overcompensates the direct biotic effect of changing biological rates (isolated in CTRL_IMPOSE) on TOU and oxygen concentrations, as evident from COUPLED_SST (Fig. 1). In all three cases (COUPLED_SST, CTRL_IMPOSE, COUPLED_IMPOSE) ΔTOU is a very good measure of $\Delta F_{O_2}^{\text{biotic}}$, the biotic component of changing air-sea O_2 -fluxes (Fig. 1, 2).

Using a larger number of transient model simulations (for details see Tab. S1) we find very good agreement between the change of the global TOU inventory between 1770 and 2100 (ΔTOU) and the cumulative biogenic oxygen air-sea exchange ($\Delta F_{O_2}^{\text{biotic}}$) (Fig. 3a). When TOU increases $\Delta F_{O_2}^{\text{biotic}}$ is negative and vice versa. The dashed line in Fig. 3a indicates the line of perfect agreement between the simulated changes in TOU and cumulative $\Delta F_{O_2}^{\text{biotic}}$. For the same model runs, there is basically no meaningful relationship between the cumulative changes in export production (ΔEP) and $\Delta F_{O_2}^{\text{biotic}}$, respectively (Fig. 3b). Almost all data points are very far from the 1:1 relationship, which in this plot represents the theoretical case that (only) changes in export production would cause an oxygen flux at the air-sea boundary (i.e. increasing export production would cause an oxygen flux out of the ocean). Actually, for many model runs (indicated by the grey hatched area), even the sign of change of export production and that of the simulated biogenic oxygen air-sea flux do not agree.

The change in export production hence turns out to be an unreliable measure of the transient development of the biogenic O_2 -flux at the ocean atmosphere boundary, while the change in TOU represents it almost perfectly. This holds for the standard simulation (COUPLED_SST, thick black + in Fig. 2), sensitivity runs with differing circulations (small black +), runs where the circulation is as in CTRL, but changing biological rates are imposed globally (blue triangle) or in specific regions (blue numbers, see Tab. S1 for details), as well as for runs in which circulation changes affect the accumulation of the TOU tracer and of oxygen, but biological rates from CTRL are assimilated at model run time either globally (red triangle) or in specific regions (red numbers, see Tab. S1 for details).

5. Discussion

By a suite of idealised model experiments we cover a wide range of possible future export production and TOU changes and circulation states. We find the robust result that the change in global TOU provides a reliable quantitative measure of the oxygen fluxes at the air-sea boundary which are induced by changes of the BCP. At the same time, change in export production does not inform about the influence of the BCP on the atmosphere. This is consistent with the finding from idealised steady state model simulations [Gnanadesikan and Marinov, 2008] and related to a strong regional decoupling of the export of organic matter and its impact on the storage of its degradation products [DeVries *et al.*, 2012; Marinov *et al.*, 2006]. It is shown here for the first time that this also holds for transient model simulations under a business-as-usual climate change scenario.

Measuring export production in the ocean is an ambitious task. There is large regional and temporal variability requiring extremely dense measurement coverage and there are notorious technical issues plaguing the methods to sample sinking particles quantitatively [Scholten *et al.*, 2001] and without biases [Kähler and Bauerfeind, 2001]. Additionally, accounting for the contribution of DOM to export [Hansell *et al.*, 2002] is difficult. Accordingly, monitoring changes of export production appears to be extremely challenging for the real ocean. With respect to biotically induced air-sea fluxes of O₂ (and CO₂, s.b.), we may be lucky that there is no need to monitor export production since it is no suitable measure of biological pump change anyway.

In contrast, computing AOU from high-quality data of temperature, salinity and oxygen is a more straight-forward task [García and Gordon, 1992]. Data archives hold a huge body of historical data [García *et al.*, 2014] which allow to derive a present-day state estimate of marine AOU [García *et al.*, 2005] and further allow to quantify its change over the last 50 yrs [Schmidt *et al.*, 2017]. Currently existing and deployed technology of oxygen-sensor equipped Argo floats [Jayne *et al.*, 2017; Johnson *et al.*, 2009] is available to quantify and monitor changes in oxygen and AOU in the future. Model studies [Duteil *et al.*, 2013; Ito *et al.*, 2004] have indicated that AOU may overestimate TOU globally by up to 25%, due to incomplete equilibration at the formation time of deep water [Körtzinger *et al.*, 2004; Wolf *et al.*, 2018]. In our model experiments, the change in AOU and the change in TOU are highly

correlated (Fig. S5), though ΔAOU tends to underestimate ΔTOU in the COUPLED model experiment by 25%. This appears to be related to a change in polar sea ice cover which can prevent complete equilibration of surface sea water with the atmosphere, a major reason identified for O_2^{sat} (AOU) to overestimate O_2^{pre} (TOU) [Duteil *et al.*, 2013; Ito *et al.*, 2004]. Polar sea ice cover is projected to decrease during the 21st century for high emission scenarios, like the one used here (RCP 8.5) (Fig. S6), which should have the effect to make AOU (O_2^{sat}) a more reliable estimate of TOU (O_2^{pre}) over the course of our model experiments. The smaller change in AOU compared to TOU in our experiments is hence an artefact of the default procedure to compute AOU (the O_2^{sat} assumption; Fig. S7). Improved procedures, e.g. the evaluated oxygen utilization, EOU [Duteil *et al.*, 2013], may be used instead. The strong correlation between ΔTOU and $\Delta\text{F}_{\text{O}_2}^{\text{biotic}}$ (Fig. 3a) as well the correlation between ΔAOU and ΔTOU (Fig. S5) suggest that changes of AOU (eventually EOU) monitored from a continued Argo float program with oxygen sensors provides the unique opportunity to monitor changes of the biological pump in the ocean and its influence on the atmosphere.

v 1.7.20, wk

6. Conclusions and outlook

Re-emphasizing the original proposal of [Volk and Hoffert, 1985] that the biological carbon pump can be best quantified by its contribution to the vertical surface-to-bottom DIC gradient, we here showed that the effect of transient changes of this pump on the atmosphere is best quantified by changes of AOU, a property directly related to that DIC gradient and easily measured in the ocean. In contrast, we found that changes of export production show no clear relationship with the biogenic O_2 -flux between atmosphere and ocean and hence has no predictive capacity to quantify relevant changes of the biological pump.

This study addresses the feedback of the biological carbon pump to the atmosphere in terms of an air-sea oxygen flux. Of real interest is the associated carbon flux. Biogenic oxygen fluxes between the ocean and the atmosphere are directly related to a stoichiometrically equivalent potential CO_2 flux of biogenic origin, which can be easily computed by dividing

the biogenic oxygen flux by the ocean mean oxygen-to-carbon ratio (the oxygen demand of organic matter degradation, $r_{-O_2:C}=1.4$; [Anderson and Sarmiento, 1994]). The true CO₂ flux attributable to changes of the biological-physical pump, will, however, be considerably different. This is due to the buffering effect of surface ocean seawater [Ito and Follows, 2005]. In steady state, the true CO₂-flux from biological pump changes may be only 10-20% of the potential CO₂-flux [Gruber et al., 2004].

We derive a first-order estimate of the steady-state CO₂-flux attributable to biological carbon pump changes from the observed rate of ocean deoxygenation [Schmidtke et al., 2017]. Over the recent 50 years the rate of ocean deoxygenation (961 Tmol per decade, [Schmidtke et al., 2017]) is mainly due to an increase in AOU (831 Tmol per decade), which is equivalent to a potential CO₂-flux into the ocean of +594 Tmol C per decade. Using the steady-state buffer correction of this flux taken from [Gruber et al., 2004] this translates into an ultimate true CO₂-flux into the ocean attributable to the biological pump of 0.7 to 1.4 Gt C per decade, or 0.07 to 0.14 Gt C/yr. Compared with the mean total marine uptake for 2006 to 2015 (2.6 ± 0.5 GtC/yr, [Le Quéré et al., 2016]) this estimate of the CO₂-flux attributable to changes of the biological carbon pump (soft tissue pump) appears negligible.

7. Acknowledgement

We acknowledge discussions with colleagues from the Biogeochemistry Modelling research units at GEOMAR. It was a discussion with our colleague Ulf Riebesell (GEOMAR) which stimulated the development of the modelling approach used in this study. W.K. acknowledges funding from German BMBF, Project BIOACID (FKZ 03F0728A). This is a contribution to the Collaborative Research Centre SFB 754, funded by the German Research Foundation (DFG).

8. Data availability

Model output is available from data.geomar.de (<http://hdl.handle.net/20.500.12085/396970fe-3529-430c-a774-55ccc681795e>).

9. Author contributions

W.K. designed the study, carried out the model experiments and analysis, and wrote the original manuscript . All authors contributed to discussion and writing of the final publication.

10. References

References from Supp. Material

Anderson, L. A., and J. L. Sarmiento (1994), Redfield ratios of remineralization determined by nutrient data analysis, *Global Biogeochem. Cycles*, 8, 65-80.

Barange, M., M. Butenschön, A. Yool, N. Beaumont, J. A. Fernandes, A. P. Martin, and J. I. Allen (2017), The cost of reducing the North Atlantic Ocean biological carbon pump, *Frontiers in Marine Science*, 3(JAN).

Bernardello, R., I. Marinov, J. B. Palter, J. L. Sarmiento, E. D. Galbraith, and R. D. Slater (2014), Response of the Ocean Natural Carbon Storage to Projected Twenty-First-Century Climate Change, *J Climate*, 27(5), 2033-2053.

Bopp, L., C. Le Quéré, M. Heimann, A. C. Manning, and P. Monfray (2002), Climate-induced oceanic oxygen fluxes: implications for the contemporary carbon budget, *Global Biogeochemical Cycles*, 16(2), doi: 10.1029/2001gb001445.

Bopp, L., L. Resplandy, A. Untersee, P. Le Mezo, and M. Kageyama (2017), Ocean (de) oxygenation from the Last Glacial Maximum to the twenty-first century: insights from Earth System models, *Philos T R Soc A*, 375(2102).

Bopp, L., et al. (2013), Multiple stressors of ocean ecosystems in the 21st century: projections with CMIP5 models, *Biogeosciences*, 10(10), 6225-6245.

Boyd, P. W., and T. W. Trull (2007), Understanding the export of biogenic particles in oceanic waters: is there consensus?, *Prog. Oceanogr.*, 72, 276-312.

Buesseler, K. O. (1998), The decoupling of production and particulate export in the surface ocean, *Global Biogeochem. Cycles*, 12, 297-310.

Cabre, A., I. Marinov, and S. Leung (2015), Consistent global responses of marine ecosystems to future climate change across the IPCC AR5 earth system models, *Climate Dynamics*, 45(5-6), 1253-1280.

Crutzen, P. J. (2002a), Geology of mankind, *Nature*, 415(6867), 23-23.

Crutzen, P. J. (2002b), The "anthropocene", *J Phys Iv*, 12(Pr10), 1-5.

DeVries, T., F. Primeau, and C. Deutsch (2012), The sequestration efficiency of the biological pump, *Geophysical Research Letters*, 39, doi:10.1029/2012GL051963.

404 Duteil, O., and A. Oschlies (2011), Sensitivity of simulated extent and future evolution of
 405 marine suboxia to mixing intensity, *Geophys. Res. Lett.*, *38*, L06607, doi:
 406 10.1029/2011GL046877.

407 Duteil, O., W. Koeve, A. Oschlies, D. Bianchi, E. Galbraith, I. Kriest, and R. Matear (2013), A
 408 novel estimate of ocean oxygen utilisation points to a reduced rate of respiration in the
 409 ocean interior, *Biogeosciences*, *10*, 7723-7738; doi: 10.5194/bg-7710-7723-2013.

410 Eppley, R. W., and B. J. Peterson (1979), Particulate organic matter flux and planktonic new
 411 production in the deep ocean, *Nature*, *282*, 677-680.

412 Garcia, H. E., T. P. Boyer, S. Levitus, R. A. Locarnini, and J. I. Antonov (2005), Climatological
 413 annual cycle of upper ocean oxygen content anomaly, *Geophys. Res. Lett.*, *32*,
 414 L05611, doi:10.1029/2004GL021745.

415 García, H. E., and L. I. Gordon (1992), Oxygen solubility in seawater: better fitting equations,
 416 *Limnol. Oceanogr.*, *37*, 1307-1312.

417 García, H. E., R. A. Locarnini, T. P. Boyer, J. I. Antonov, O. K. Baranova, M. M. Zweng, J. R.
 418 Reagan, and D. R. Johnson (2014), *World Ocean Atlas 2013, Volume 3: Dissolved Oxygen,*
 419 *Apparent Oxygen Utilization, and Oxygen Saturation.*

420 Gnanadesikan, A., and I. Marinov (2008), Export is not enough: nutrient cycling and carbon
 421 sequestration, *Mar. Ecol. Prog. Ser.*, *364*, 289-294.

422 Gruber, N., P. Friedlingstein, C. B. Field, R. Valentini, M. Heimann, J. E. Richey, P. Romero
 423 Lankao, D. Schulz-Bull, and C.-T. Chen (2004), The Vulnerability of the Carbon Cycle in the
 424 21st Century: An Assessment of Carbon-Climate-Human Interactions, in *The Global Carbon*
 425 *Cycle: Integrating Humans, Climate, and the Natural World*, edited by C. B. F. a. M. R.
 426 Raupach, pp. 45-76, Island Press, Washington DC.

427 Hansell, D. A., C. A. Carlson, and Y. Suzuki (2002), Dissolved organic carbon export with North
 428 Pacific Intermediate Water formation, *Global Biogeochem. Cycles*, *16*,
 429 10.1029/2000GB001361.

430 Harrison, C. S., M. C. Long, N. S. Lovenduski, and J. K. Moore (2018), Mesoscale Effects on
 431 Carbon Export: A Global Perspective, *Global Biogeochemical Cycles*, *32*(4), 680-703.

432 Henson, S. A., R. Sanders, and E. Madsen (2012), Global patterns in efficiency of particulate
 433 organic carbon export and transfer to the deep ocean, *Global Biogeochem. Cy*, *26*, GB1028,
 434 doi:10.1029/2011GB004099.

435 Henson, S. A., R. Sanders, E. Madsen, P. J. Morris, F. Le Moigne, and G. D. Quartly (2011), A
 436 reduced estimate of the strength of the ocean's biological carbon pump, *Geophys. Res. Lett.*,
 437 *38*, L04606, doi:10.1029/2011GL046735.

438 Hoegh-Guldberg, O., R. Cai, E. S. Poloczanska, P. Brewer, S. Sundby, K. Hilmi, V. J. Fabry, and
 439 J. S (2014), The ocean, in *Climate Change 2014: Impacts, Adaptation, and Vulnerability. Part*
 440 *B: Regional Aspects. Contribution of Working Group II to the Fifth Assessment Report of the*

441 *Intergovernmental Panel on Climate Change*, edited by V. R. Barros, et al., pp. 1655-1731,
 442 Cambridge University Press, Cambridge, United Kingdom and New York, NY, USA.

443 Ito, T., and M. J. Follows (2005), Preformed phosphate, soft tissue pump and atmospheric
 444 CO₂, *J. Mar. Res.*, **63**, 813-839.

445 Ito, T., M. J. Follows, and E. A. Boyle (2004), Is AOU a good measure of respiration in the
 446 ocean?, *Geophys. Res. Lett.*, **31**, L17305, doi: 10.1029/2004GL020900.

447 Ito, T., S. Minobe, M. C. Long, and C. Deutsch (2017), Upper ocean O₂ trends: 1958-2015,
 448 *Geophysical Research Letters*, **44**(9), 4214-4223.

449 Jayne, S. R., D. Roemmich, N. Zilberman, S. C. Riser, K. S. Johnson, G. C. Johnson, and S. R.
 450 Piotrowicz (2017), The Argo Program Present and Future, *Oceanography*, **30**(2), 18-28.

451 Johnson, K. S., W. M. Berelson, E. S. Boss, Z. Chase, H. Claustre, S. R. Emerson, N. Gruber, A.
 452 Kortzinger, M. J. Perry, and S. C. Riser (2009), Observing Biogeochemical Cycles at Global
 453 Scales with Profiling Floats and Gliders Prospects for a Global Array, *Oceanography*, **22**(3),
 454 216-225.

455 Kähler, P., and E. Bauerfeind (2001), Organic particles in a shallow sediment trap: substantial
 456 loss to the dissolved phase, *Limnol. Oceanogr.*, **46**, 719-723.

457 Keeling, R. F., A. Körtzinger, and N. Gruber (2010), Ocean deoxygenation in a warming world,
 458 *Annu. Rev. Marine. Sci.*, **2**, 199-229.

459 Keller, D., A. Oschlies, and M. Eby (2012), A new marine ecosystem model for the University
 460 of Victoria Earth System Climate Model, *Geosci. Model Dev.*, **5**, 1195-1220, doi:
 461 10.5194/tmd-1195-1195-2012.

462 Koeve, W. (2001), Wintertime nutrients in the North Atlantic - New approaches and
 463 implications for estimates of seasonal new production, *Marine Chemistry*, **74**, 245-260.

464 Koeve, W., and P. Kähler (2016), Oxygen utilization rate (OUR) underestimates ocean
 465 respiration: A model study, *Global Biogeochemical Cycles*, **30**(8), 1166-1182.

466 Koeve, W., H. Wagner, P. Kähler, and A. Oschlies (2015), ¹⁴C-age tracers in global ocean
 467 circulation models, *Geosci. Model Dev.*, **8**, 2079-2094.

468 Körtzinger, A., L. Mintrop, and J. C. Duinker (1998), On the penetration of anthropogenic CO₂
 469 into the North Atlantic Ocean, *J. Geophys. Res.*, **103**, 18681-18689.

470 Körtzinger, A., J. Schimanski, U. Send, and D. Wallace (2004), The ocean takes a deep breath,
 471 *Science*, **306**, 1337.

472 Kwon, E. Y., F. Primeau, and J. L. Sarmiento (2009), The impact of remineralization depth on
 473 the air-sea carbon balance, *Nature Geoscience*, **2**, 630-635.

474 Kwon, E. Y., J. L. Sarmiento, J. R. Toggweiler, and T. DeVries (2011), The control of
 475 atmospheric pCO₂ by ocean ventilation change: The effect of the oceanic storage of
 476 biogenic carbon, *Global Biogeochemical Cycles*, **25**.

477 Lampitt, R. S., E. P. Achterberg, T. R. Anderson, and a. others (2008), Ocean fertilization: a
 478 potential means of geoengineering?, *Phil. Trans. R. Soc. A*, 366, doi:10.1098/rsta.2008.0139.

479 Laufkötter, C., et al. (2016), Projected decreases in future marine export production: the role
 480 of the carbon flux through the upper ocean ecosystem, *Biogeosciences*, 13(13), 4023-4047.

481 Laufkötter, C., et al. (2015), Drivers and uncertainties of future global marine primary
 482 production in marine ecosystem models, *Biogeosciences*, 12(23), 6955-6984.

483 Laws, E. A., P. G. Falkowski, W. O. Smith, H. Ducklow, and J. J. McCarthy (2000), Temperature
 484 effects on export production in the open ocean, *Global Biogeochem. Cycles*, 14, 1231-1246.

485 Le Quéré, C., et al. (2016), Global Carbon Budget 2016, *Earth System Science Data*, 8(2), 605-
 486 649.

487 Marinov, I., A. Gnanadesikan, J. R. Toggweiler, and J. L. Sarmiento (2006), The Southern
 488 Ocean biogeochemical divide, *Nature*, 441, 964-967.

489 Meinshausen, M., et al. (2011), The RCP greenhouse gas concentrations and their extensions
 490 from 1765 to 2300, *Climatic Change*, 109(1-2), 213-241.

491 Oschlies, A., W. Koeve, A. Landolfi, and P. Kahler (2019), Loss of fixed nitrogen causes net
 492 oxygen gain in a warmer future ocean, *Nat Commun*, 10.

493 Peng, T. H., R. Wanninkhof, J. L. Bullister, R. A. Feely, and T. Takahashi (1998), Quantification
 494 of decadal anthropogenic CO₂ uptake in the ocean based on dissolved inorganic carbon
 495 measurements, *Nature*, 396(6711), 560-563.

496 Resplandy, L. (2018), Climate change and oxygen in the ocean, *Nature*, 557(7705), 314-315.

497 Sarmiento, J. L., and N. Gruber (2006), *Ocean biogeochemical dynamics*, Princeton University
 498 Press, Princeton.

499 Sarmiento, J. L., T. M. C. Hughes, R. J. Stouffer, and S. Manabe (1998), Simulated response of
 500 the ocean carbon cycle to anthropogenic climate warming, *Nature*, 393, 245-249.

501 Schmidtko, S., L. Stramma, and M. Visbeck (2017), Decline in global oceanic oxygen content
 502 during the past five decades, *Nature*, 542(7641), 335-339.

503 Scholten, J. C., J. Fietzke, S. Vogler, M. Rutgers van der Loeff, A. Mangini, W. Koeve, J.
 504 Waniek, P. Stoffers, A. Antia, and J. Kuss (2001), Trapping efficiency of sediment traps from
 505 the deep eastern North Atlantic: the 230Th calibration, *Deep-Sea Res. Pt. II*, 48, 2383-2408.

506 Shaffer, G., S. M. Olsen, and J. O. P. Pedersen (2009), Long-term ocean oxygen depletion in
 507 response to carbon dioxide emissions from fossil fuels, *Nature Geoscience*, 2(2), 105-109.

508 Steffen, W., J. Grinevald, P. Crutzen, and J. McNeill (2011), The Anthropocene: conceptual
 509 and historical perspectives, *Philos T R Soc A*, 369(1938), 842-867.

510 Taucher, J., and A. Oschlies (2011), Can we predict the direction of marine primary
511 production change under global warming?, *Geophysical Research Letters*, 38, doi:
512 10.1029/2010gl045934.

513 Volk, T., and M. I. Hoffert (1985), Ocean carbon pumps, analysis of relative strengths and
514 efficiencies in ocean-driven atmosphere CO₂ changes, in *The carbon cycle and atmospheric*
515 *CO₂: natural variations archean to present*, edited by E. T. Sundquist and W. S. Broecker, pp.
516 99-110, Geophysical Monographs, AGU, Washington, D.C.

517 Weaver, A. J., et al. (2001), The UVic earth system climate model: model description,
518 climatology, and applications to past, present and future climates, *Atmosph. Oceans*, 39,
519 361-428.

520 Wolf, M. K., R. C. Hamme, D. Gilbert, I. Yashayaev, and V. Thierry (2018), Oxygen Saturation
521 Surrounding Deep Water Formation Events in the Labrador Sea From Argo-O-2 Data, *Global*
522 *Biogeochemical Cycles*, 32(4), 635-653.

523 Yamamoto, A., A. Abe-Ouchi, M. Shigemitsu, A. Oka, K. Takahashi, R. Ohgaito, and Y.
524 Yamanaka (2015), Global deep ocean oxygenation by enhanced ventilation in the Southern
525 Ocean under long-term global warming, *Global Biogeochemical Cycles*, 29(10), 1801-1815.

526 Yool, A., A. P. Martin, C. Fernandez, and D. R. Clark (2007), The significance of nitrification for
527 oceanic new production, *Nature*, 447(7147), 999-1002.

528
529
530
531
532
533

11. Figures (captions):

Fig. 1. Theoretical and simulated cumulative global oxygen fluxes (Pmol O₂) in UVic model experiment COUPLED_SST (solid lines) and COUPLED (dashed lines) between 1770 and 2100. Simulated air-sea oxygen flux ($\Delta F_{O_2}^{biotic}$, black solid line), theoretical cumulative flux (green lines) derived from cumulative export-production change (**Fig. S3b**), and theoretical air-sea flux derived from TOU inventory change (red lines, **Fig. S3b**). Theoretical fluxes are computed assuming that the changes in cumulative export or TOU, respectively, result in an immediate flux at the air-sea boundary. Following conventions, a flux into the ocean is positive. TOU is integrated below $z=130\text{m}$, export production is quantified at $z=130\text{m}$.

Fig 2. Disentangling direct and indirect effects of the biological-physical carbon pump changes on oxygen and TOU inventory as well as oxygen fluxes. All numbers are presented in units of oxygen flux at the air sea boundary. **(a)** Experiment CTRL_IMPOSE (no circulation change, but with imposed changes of biological rates affecting O₂-sms like in the COUPLED, compare Fig. S4a): simulated oxygen air-sea flux $\Delta F_{O_2}^{biotic}$ (black), change in oxygen inventory (blue), theoretical air-sea flux derived from change in TOU inventory (dashed red), cumulative theoretical O₂-flux (green) derived from cumulative change in export production, cumulative theoretical O₂-flux (orange) derived from cumulative change of respiration below 1000m (so called sequestration flux). **(b)** Experiment COUPLED_IMPOSE (circulation change affects oxygen and TOU, but biological rates affecting O₂-sms are like in CTRL; compare Fig. S4b). Theoretical fluxes are computed assuming that the changes in cumulative export, sequestration flux, or TOU, respectively, result in a flux at the air-sea boundary without any time delay. Following conventions, a flux into the ocean is positive. Inventory changes of O₂ and TOU are global integrals, export production is quantified at $z=130\text{m}$.

Fig. 3. Time integrated (yr 1765 to 2100) change of **(a)** TOU and **(b)** export production (in oxygen equivalents) vs. the cumulative biogenic air-sea oxygen flux. Dashed lines indicate the respective equivalence points (1:1 relationship) of (a) ΔTOU vs $\Delta F_{O_2}^{biotic}$ and (b) ΔEP and $\Delta F_{O_2}^{biotic}$, assuming that changes in TOU or EP would translate completely and immediately into a O₂- flux at the sea surface. The hatched area indicates

566 where the signs of change of ΔEP and $\Delta F_{O_2}^{biotic}$ are inconsistent. Compare **Tab. S1** for symbol
567 legend.
568

Figure.

Fig. 1

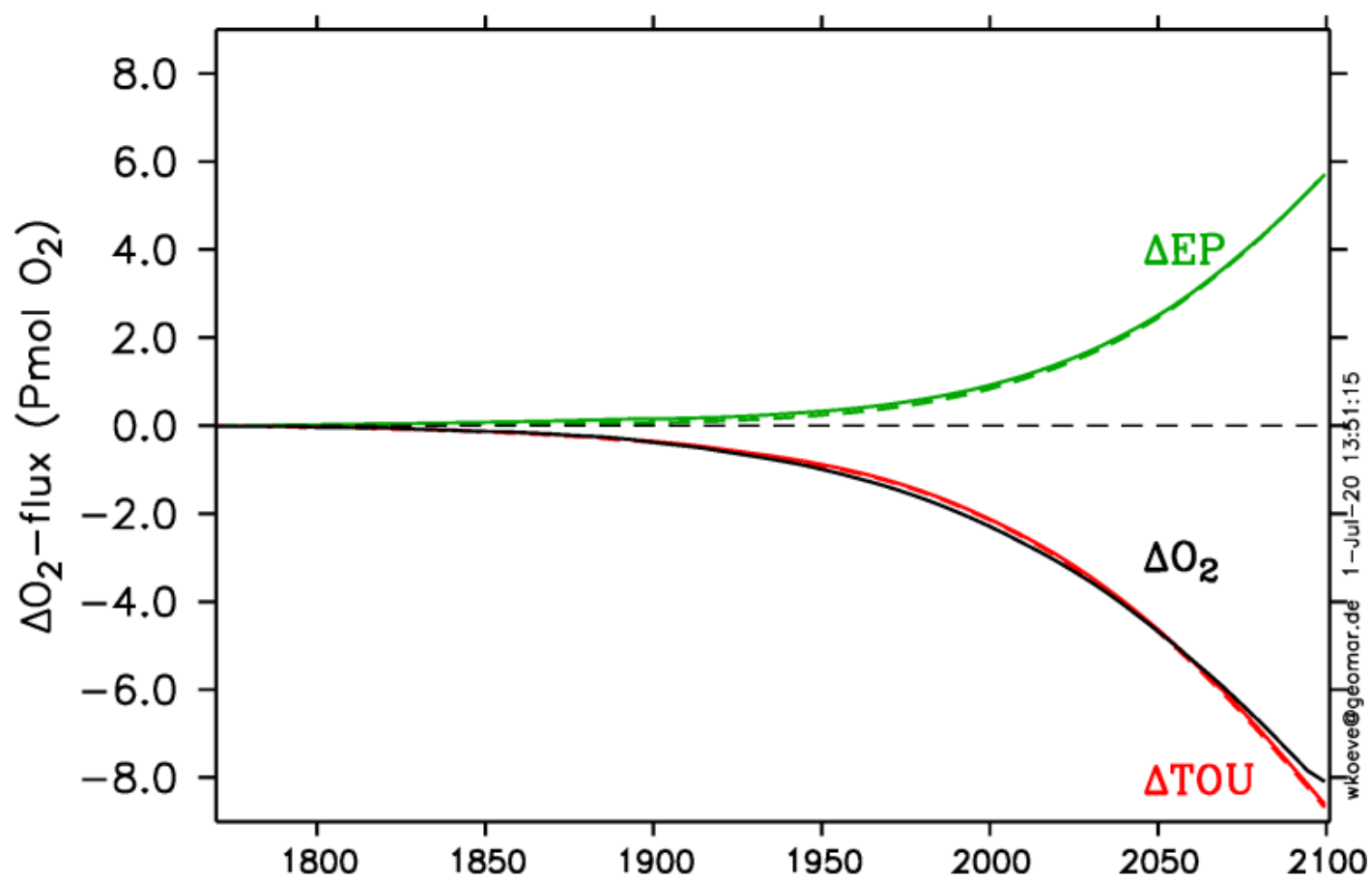


Figure.

Fig. 2

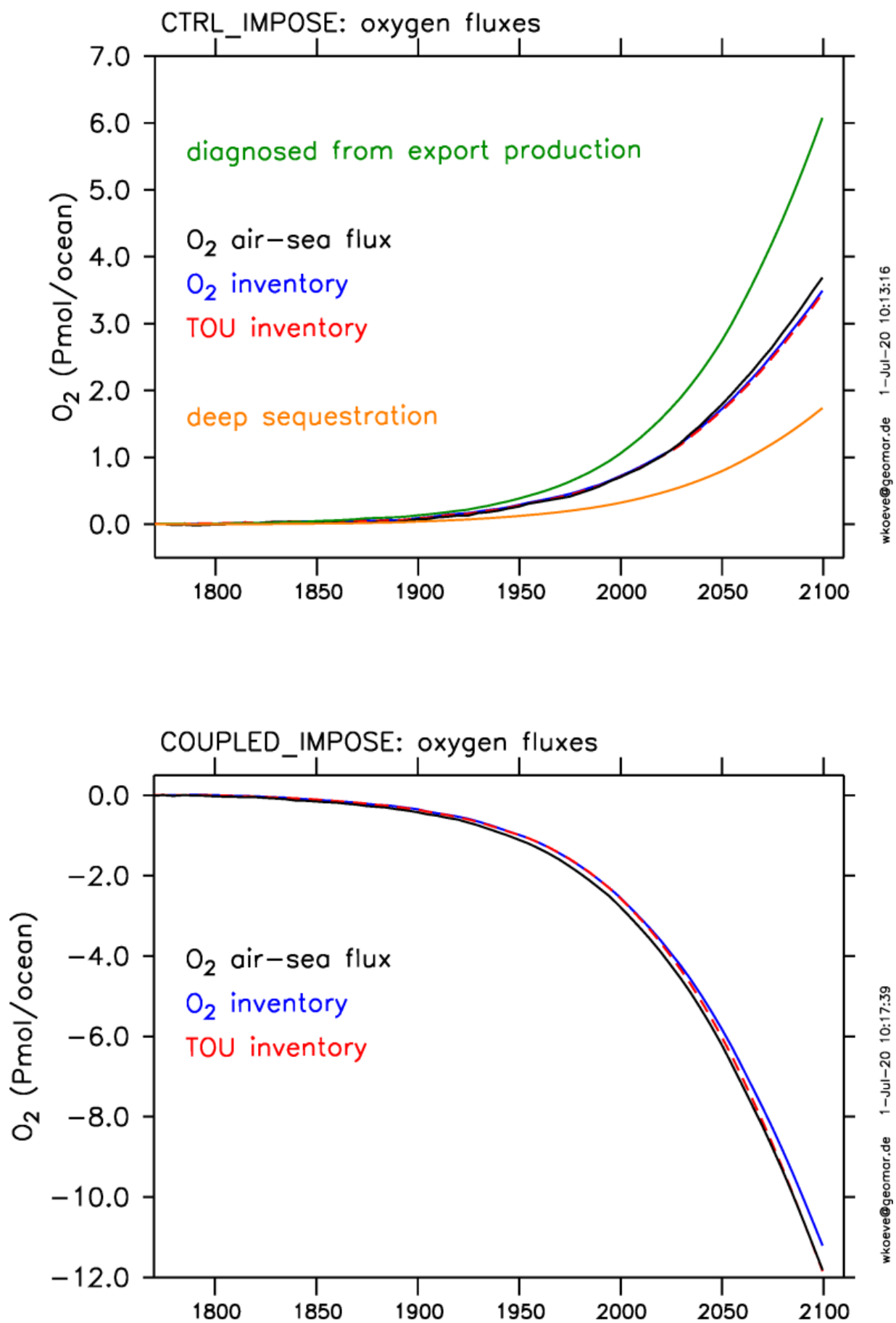
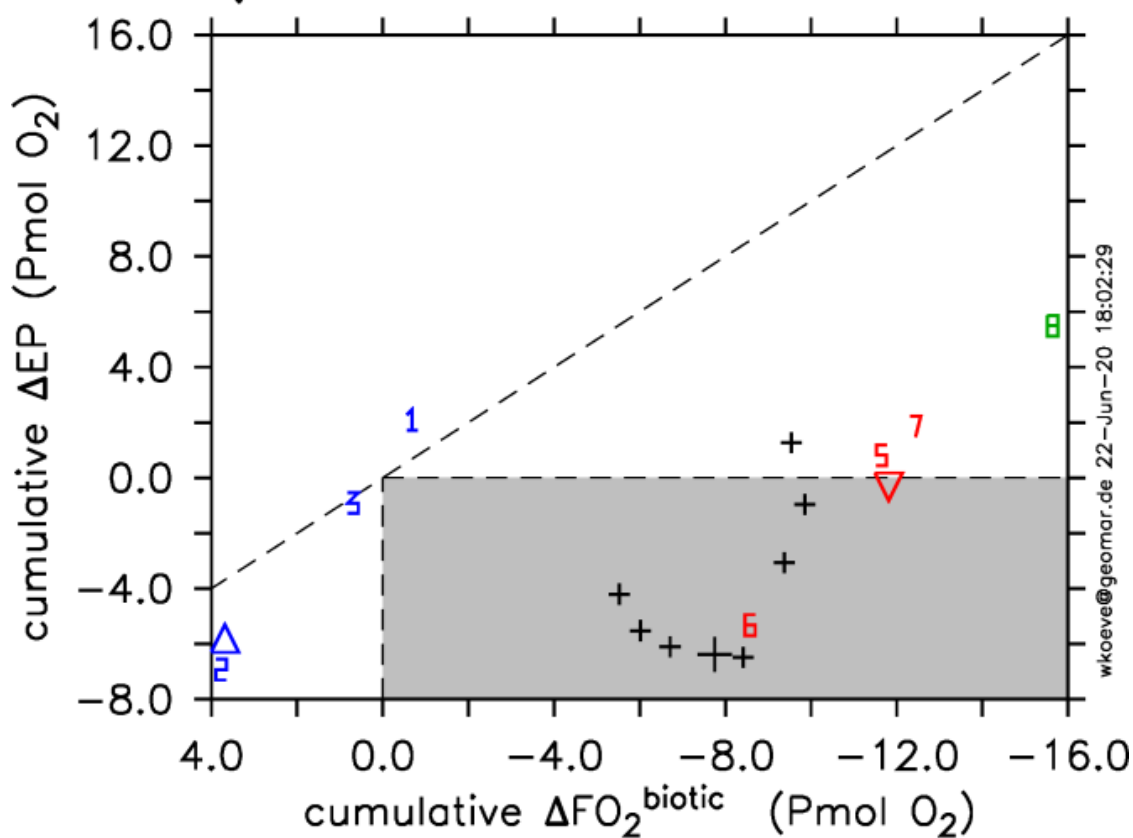
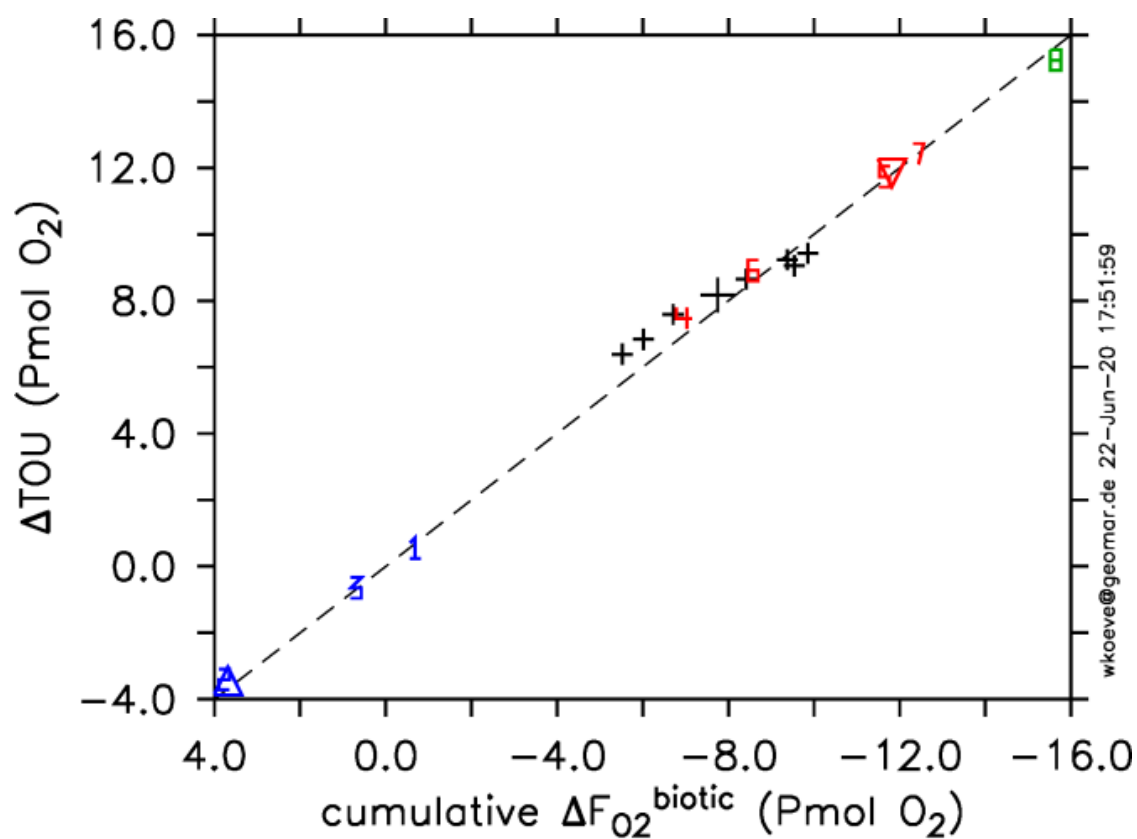


Figure.

Fig. 3



Does export production measure transient changes of the biological carbon pump under global warming?

Koeve, W., Kähler, P., Oschlies, A.

[Biogeochemical Modelling, Helmholtz-Zentrum für Meeresforschung Kiel (GEOMAR), Kiel, Germany]

Contents of this file

Text S1
Figures S1 to S7
Tables S1 to S2

Introduction

Here we provide Supplementary Methods (Text S1), Supplementary Figures (S1 to S7) which present details of our model experiments and two Supplementary Tables.

Text S1.

Supplementary Methods

UVic model

All transient (yr 1765 to 2100) model runs presented in this paper are simulated with an ocean-sea-ice-atmosphere version of the University of Victoria Earth System Model of intermediate complexity (UVic) version 2.9 [Keller *et al.*, 2012; Weaver *et al.*, 2001] supplemented with idealised tracers of true oxygen utilization (TOU; [Ito *et al.*, 2004; Koeve and Kähler, 2016]) and ideal age [England, 1995; Koeve *et al.*, 2015]. The fully coupled Earth System model was spun up under constant Holocene conditions ($p\text{CO}_2=278$, orbital forcing of yr 1765), thereafter the land model was turned off and a 1500 yr drift run was performed with the oceanic (incl. sea ice) and atmospheric model with prescribed monthly mean wind forcing from NCAR/NCEP climatological data. Starting from the state at the end of the drift run, we perform a coupled simulation (**COUPLED**) under the RCP 8.5 business-as-usual CO_2 emission scenario, applying emissions from fossil fuels and land use change using forcing data from the RCP database (<http://www.iiasa.ac.at>; [Meinshausen *et al.*, 2011]), corrected, however, for net land fluxes diagnosed from a fully coupled UVic Earth System run. The residual CO_2 emissions (dubbed RCP85-star forcing) applied to the ocean + atmosphere model in COUPLED add up to 1970 Gt C between 1770 and 2100. We also perform a control run (**CTRL**) as a drift run (no CO_2 emissions) between yr 1765 and 2100. Atmospheric $p\text{CO}_2$ was 275.1 ± 0.05 ppm in the control run and surface air temperature was 13.02 ± 0.03 °C. The coupled atmosphere-ocean run COUPLED is characterized by a changing climate (the atmosphere warms by 3.72 °C; **Fig. S1b**), changing ocean circulation (as indicated by regional changes of the model's ideal age; **Fig. S2**) and an increase in atmospheric $p\text{CO}_2$ to 943 ppmv until yr 2100 (**Fig. S1a**). The ocean takes up a total of 542 Gt C, equivalent to 27.5% of the cumulative emissions to the atmosphere. Using the output of experiments COUPLED and CTRL, we diagnose the annual mean anomalies (COUPLED - CTRL) of sea surface temperature, SST, (x, y, and t dimensions), and oxygen sources-minus-sinks ($\text{O}_2\text{-sms}$), (x, y, z, and t dimensions). We modify the UVic code to allow for the assimilation of these anomalies and design a series of idealised experiments which combine the impact of global warming on biological rates including export and respiration and different possible intensities of warming-induced circulation changes (see Tab. S1 for details).

Experiments carried out

Starting from the experiments COUPLED and CTRL explained above and the diagnosed SST anomalies, we perform a series of experiments in which the oxygen flux between the ocean and the atmosphere does not feel the change in surface ocean temperature, hence $F_{\text{O}_2} = F_{\text{O}_2}^{\text{biotic}}$. In experiments #1 to #7 and #12 to #18, the annual mean sea surface temperature (SST) difference between COUPLED and CTRL has been assimilated at model run time for the computation of oxygen solubility and gas exchange. Air-sea oxygen flux is hence corrected for the solubility effect of global warming. Runs 8-11 have the physical conditions of CTRL, hence they do not need to assimilate SST for oxygen solubility explicitly.

Tab S1 gives an overview of the experiments carried out. We construct a range of potential responses of the biological carbon pump to climate change by combining four categories of experiments:

(a) Coupled ocean-atmosphere run (COUPLED_SST, #1 in Tab. S1, large black + in **Figs. 3, S5, S7**), in which changing biological rates as well as changing circulation both affect oxygen and TOU tracer values according to the RCP85star climate scenario. Oxygen (and TOU) sources and sinks in this run are computed prognostically.

(b) Coupled transient runs with changing climate and circulation (like in COUPLED_SST) where biological rates from CTRL are assimilated at model run time everywhere (COUPLED IMPOSE, #2 in Tab. S1) or in specified regions (experiments #3 - #6, see last column of Tab. S1 for details; red symbols in **Fig. 3, S5, S7**) are carried out. The assimilation procedure is adopted from [Bopp *et al.*, 2002; Yamamoto *et al.*, 2015], but modified as follows. The difference of local annual means (4D) of oxygen source-minus-sinks (O_2 -sms) between COUPLED and CTRL is computed offline, stored to file, and assimilated at model run time to affect the oxygen and TOU tracer. The assimilation process differs for runs with climate change (runs 2-7) in comparison to CTRL-like runs (next section). In model run #2, the assimilation is carried out in order to compensate for changes occurring at model run time and, in the annual mean, causes the effect of biological rates on oxygen and TOU to be almost identical with CTRL (**Fig. S4b**). In this run, circulation changes only affect the oxygen and TOU tracer distribution. Runs #3 to #6 are variants of run #2, in which the assimilation is only carried out in specific regions, e.g. south of 40°S (run #3). Run #7 is a specific case in which O_2 -sms is assimilated twice which provides an extreme simulation with inverted response of the biological processes on climate change.

(c) Control runs #8 to #11 (no climate change and no circulation change) to which we assimilate biological rates from COUPLED at model run time everywhere or in specified regions (dark blue symbols in **Fig. 3, S5, S7**) are carried out. Runs #8 to #11 have the climate and circulation of CTRL and assimilate the biological rate differences in order to impose the impact of transient changes of biological rates on oxygen (and the TOU tracer). In these runs only the (imposed) changes of biological rates cause the oxygen and TOU tracer distribution to change since circulation has no trend between 1770 and 2100 in CTRL. In run #8, the local annual mean difference of O_2 -sms is added to the O_2 -sms term emerging at model run time (see **Fig S4a**). In runs #9 to #11 assimilation of O_2 -sms is restricted to specific regions, e.g. south of 40°S (run #9).

d) In addition to the main experiment COUPLED_SST with default circulation (large black + in **Figs. 3, S5, S7**), we perform sensitivity experiments with modified vertical background diffusivity (# 12 to #18 in **Tab. S1**, small black + in **Figs. 3, S5, S7**). Background vertical diffusivity has been varied between 0.5 and 0.05 cm²/sec to simulate different ocean circulations similar to [Duteil and Oschlies, 2011; Koeve *et al.*, 2015]. The runs are based on respective spin-up, drift, and control runs. The annual mean anomalies of SST, derived from respective COUPLED and CTRL model experiments are assimilated at model runtime for the computation of oxygen air sea exchange.

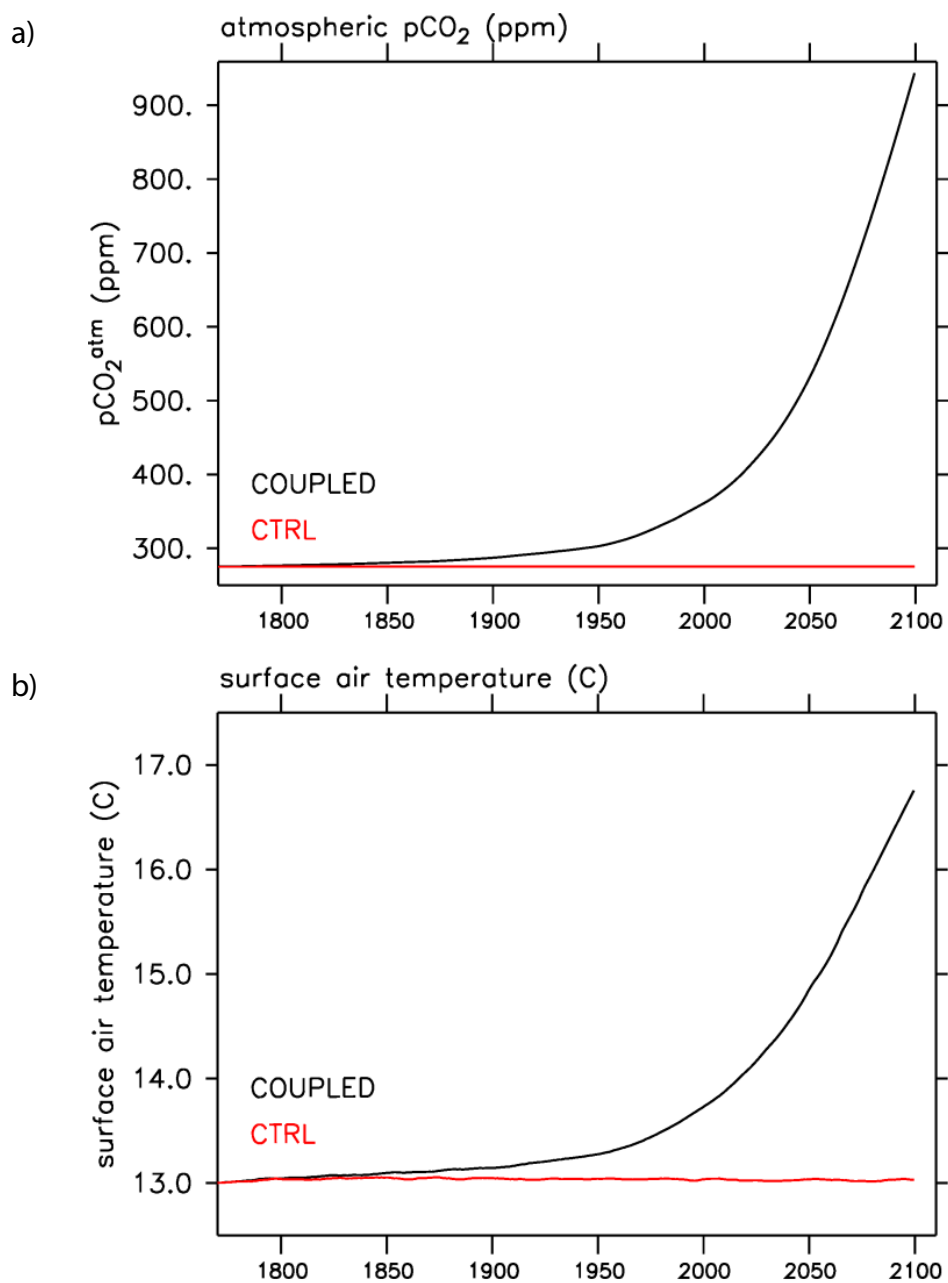


Figure S1. Transient atmospheric properties between years 1770 and 2100: (a) atmospheric $p\text{CO}_2$ (ppm) and (b) surface air temperature (°C) of run COUPLED (black solid lines) and CTRL (red solid lines).

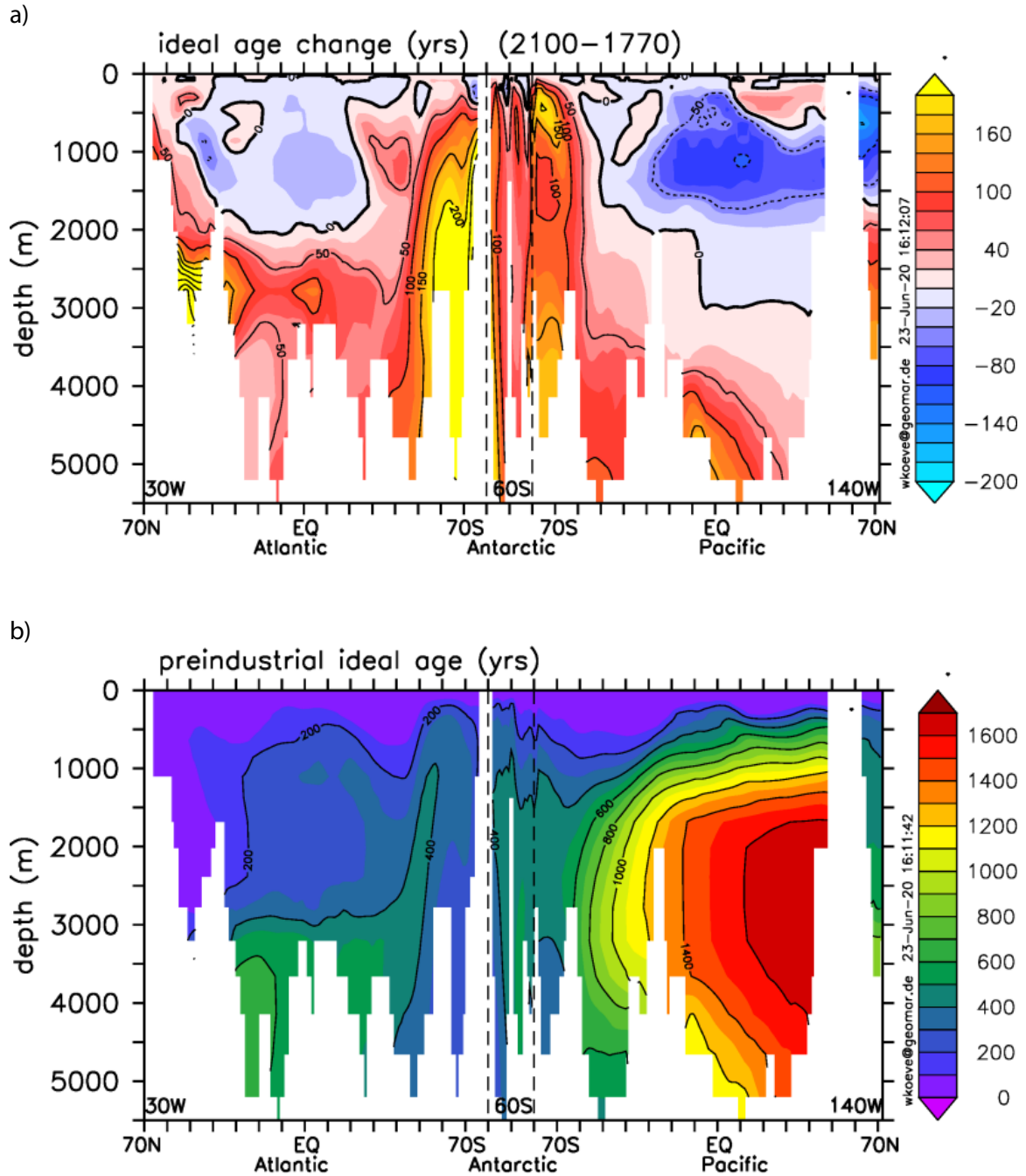


Figure S2. Ideal age (years) along a Atlantic Ocean – Southern Ocean – Pacific Ocean transect: (a) Age change in run COUPLED (2100-1770), (b) Age distribution in 1770 in run CTRL.

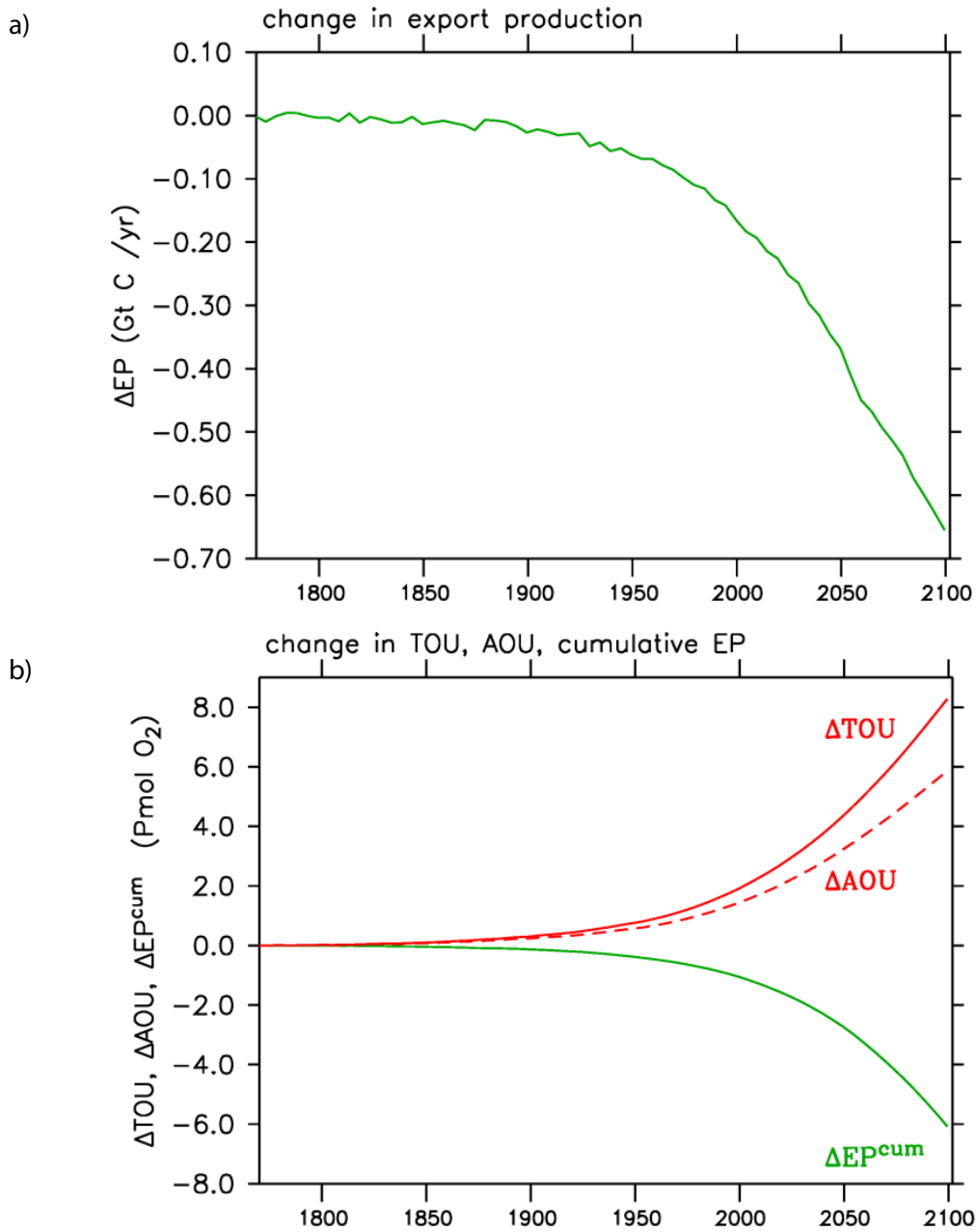


Figure S3. Transient evolution of (a) export production (Gt C / yr; $z=130m$), (b) cumulative export production (green solid), true oxygen utilization (TOU, red solid), and apparent oxygen utilization (AOU, red dashed). Note that the cumulative change in export production in (a) is presented in carbon units per year while the cumulative change in export production in (b) is given in equivalent oxygen units (Pmol O_2) to better compare against TOU and AOU changes. In (b) number given for TOU and AOU are global integrals below $z=130m$.

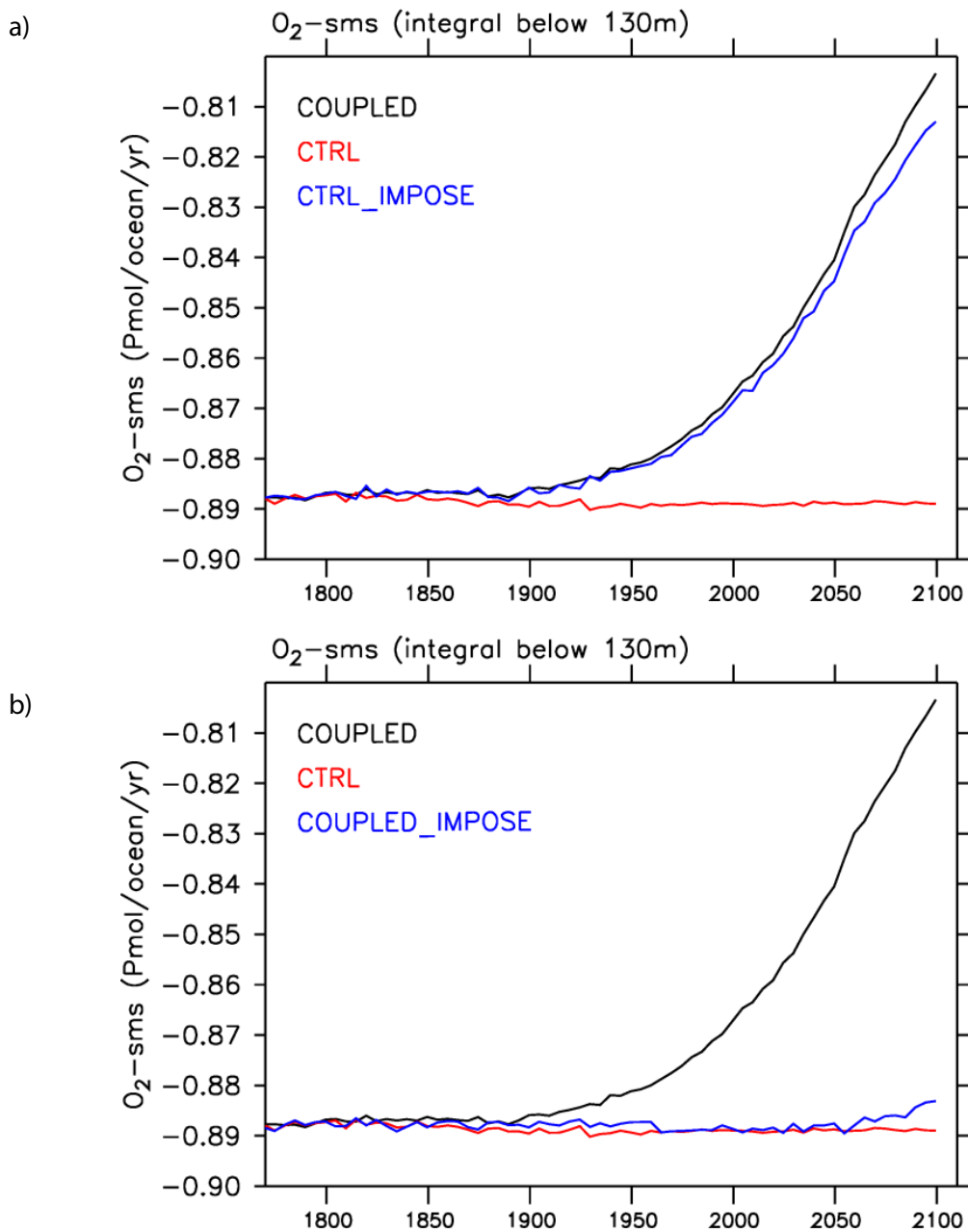


Figure S4. Globally integrated oxygen sinks-minus-sources in the ocean interior ($z > 130\text{m}$) for runs COUPLED (black), CTRL (red), CTRL_IMPOSE (blue, panel a), and COUPLED_IMPOSE (blue, panel b).

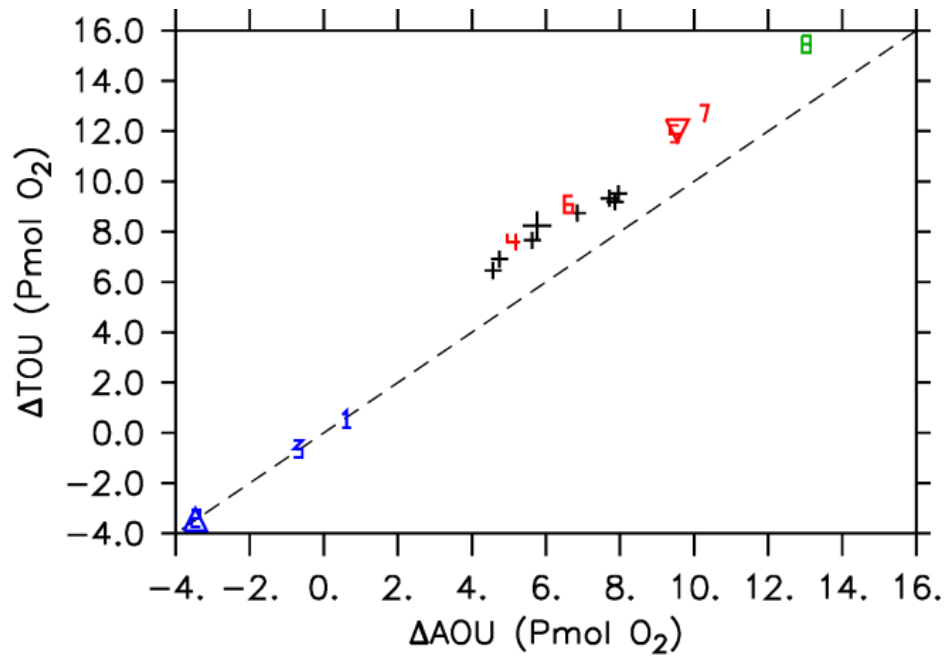


Figure S5. Transient change (2100 – 1770) of globally integrated true oxygen utilization (TOU) vs. apparent oxygen utilization (AOU) from model runs (Tab. S1) 1a to 7a, 8-11, and 12a to 18a. Note that AOU cannot be computed correctly for model runs 1-7 and 12-18 which apply SST assimilation for oxygen solubility and gas exchange computation, since the temperature at the time of gas exchange is not traced by an idealized tracer into the ocean interior in our model runs. Hence, we performed additional model runs (1a to 7a, 12a to 18a) without SST assimilation, but otherwise identical to runs 1 to 7 and 12 to 18, which are used for the comparison in this figure. Symbols are as in Fig. 2, respectively.

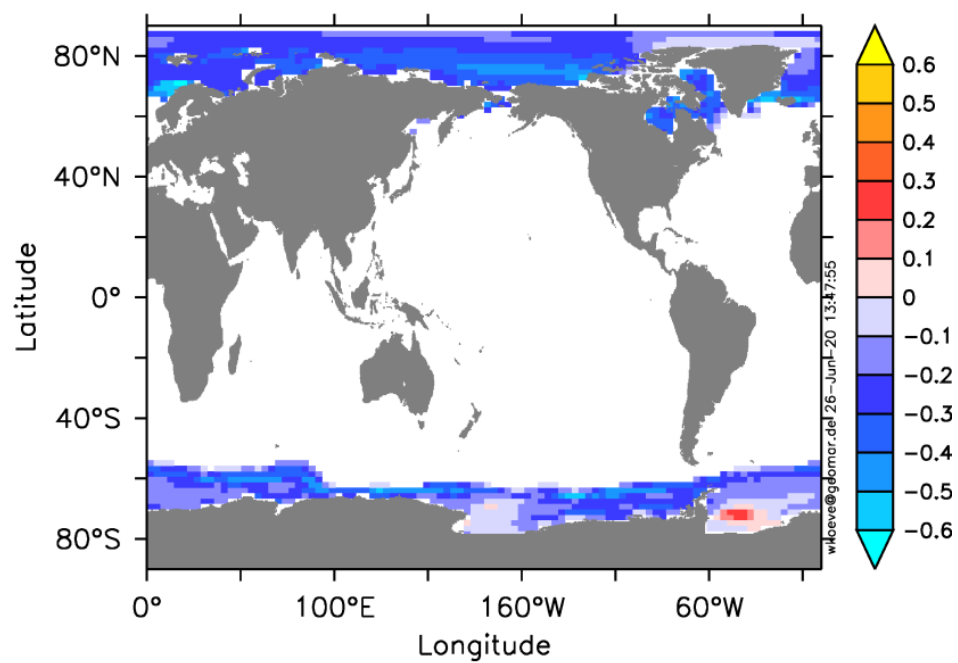


Figure S6. Change of ice cover (area fraction) between 1770 and 2100 in run COUPLED.

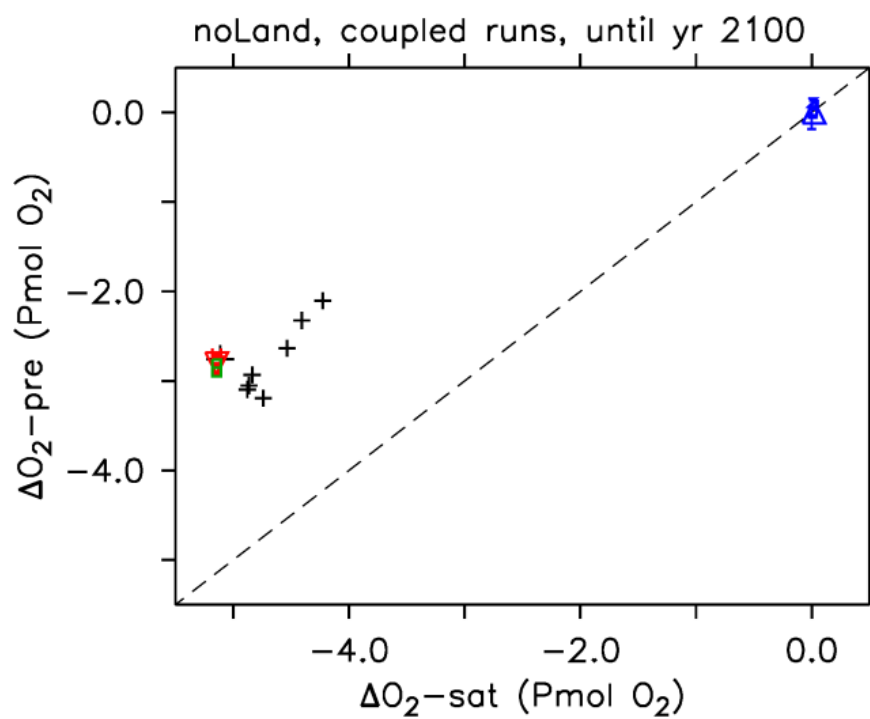


Figure S7. Transient change (2100 - 1770) of globally integrated preformed oxygen (O_2^{pre}) vs. globally integrated saturated oxygen (O_2^{sat}) from model runs 1a to 7a, 8-11,, and 12a-18a. For Details see caption of Fig. S5 and Tab. S1.

Table S1. Transient experiments carried out. We construct a range of potential responses of the biological carbon pump to climate change by combining four categories of experiments. (a) Coupled ocean-atmosphere runs (large black + in **Fig. 3**), in which changing biological rates as well as changing circulation affect oxygen and TOU tracer distribution according to the RCP85star climate scenario. (b) Coupled transient runs 2-6 with changing climate and circulation (like in COUPLED_SST) where biological rates from CTRL are assimilated at model run time everywhere or in specified regions (red symbols in **Fig. 3**). (c) Control runs 8-11 (no climate change and no circulation change) to which we assimilate biological rates from COUPLED at model run time everywhere or in specified regions (dark blue symbols in **Fig. 3**). (d) COUPLED model runs with modified background diffusivity (K_v , cm^2/sec) as indicated in column 3. SST difference to a respective control run is assimilated at model run time for the computation of oxygen solubility and gas-exchange. (See Supplementary Methods for details).

#	Symbols in Fig. 3	Run name	SST for ASE	Assimilation of biological rates
	-	COUPLED	-	-
	-	CTRL	-	-
1	large black +	COUPLED_SST	x	-
			x	-
2	red ▽	COUPLED_IMPOSE	x	x, everywhere
3	red 4	CoupAssS40	x	x, south of 40S
4	red 5	CoupAssS40N40	x	x, 40S to 40N
5	red 6	CoupAssN40	x	x, north of 40N
6	red 7	CoupAssS40no	x	x, north of 40S
7	green 8	CoupAss2x	x	x, everywhere, but twice
8	blue Δ	CTRL_IMPOSE	-	x, everywhere
9	blue 1	CtrlAssS40	-	x, south of 40S
10	blue 2	CtrlAssS40N40	-	x, 40S to 40N
11	blue 3	CtrlAssN40	-	x, north of 40N
12	small black +	$K_v = 0.5$	x	-
13	small black +	$K_v = 0.4$	x	-
14	small black +	$K_v = 0.3$	x	-
15	small black +	$K_v = 0.2$	x	-
16	small black +	$K_v = 0.1$	x	-
17	small black +	$K_v = 0.05$	x	-
18	small black +	$K_v = 0.01$	x	-

Table S2. Regional cumulative change in export production (EP) (z=130m) and the change in shallow TOU (z=130 to 1500m) between 1770 and 2100 (Pmol O₂).

Region	EP	TOU	TOU/EP
South of 40S	1.7	2.2	1.3
40S to 40N	-6.1	-1.0	0.16